

Plasma potential measurements using an emissive probe made of oxide cathode

Jian-Quan Li(李建泉), Hai-Jie Ma(马海杰), and Wen-Qi Lu(陆文琪)

Citation: Chin. Phys. B, 2024, 33 (**4**): 045205. DOI: 10.1088/1674-1056/ad1821
Journal homepage: http://cpb.iphy.ac.cn; http://iopscience.iop.org/cpb

What follows is a list of articles you may be interested in

Interaction between plasma and electromagnetic field in ion source of 10 cm ECR ion thruster

Hao Mou(牟浩), Yi-Zhou Jin(金逸舟), Juan Yang(杨涓), Xu Xia(夏旭), and Yu-Liang Fu(付瑜亮)
Chin. Phys. B, 2022, 31 (**7**): 075202. DOI: 10.1088/1674-1056/ac4906

Distribution of charged lunar dust in the south polar region of the moon

Qing Xia(夏清), Ming-Hui Cai(蔡明辉), Liang-Liang Xu(许亮亮), Rui-Long Han(韩瑞龙), Tao Yang(杨涛), and Jian-Wei Han(韩建伟)
Chin. Phys. B, 2022, 31 (**4**): 045201. DOI: 10.1088/1674-1056/ac2e61

Time-resolved radial uniformity of pulse-modulated inductively coupled O_2/Ar plasmas

Wei Liu(刘巍), Chan Xue(薛婵), Fei Gao(高飞), Yong-Xin Liu(刘永新), You-Nian Wang(王友年), and Yong-Tao Zhao(赵永涛)
Chin. Phys. B, 2021, 30 (**6**): 065202. DOI: 10.1088/1674-1056/abe3f5

Experimental and numerical investigation of a Hall thruster with a chamfered channel wall

Hong Li(李鸿), Guo-Jun Xia(夏国俊), Wei Mao(毛威), Jin-Wen Liu(刘金文), Yong-Jie Ding(丁永杰), Da-Ren Yu(于达仁), Xiao-Gang Wang(王晓钢)
Chin. Phys. B, 2018, 27 (**10**): 105209. DOI: 10.1088/1674-1056/27/10/105209

Influence of a centered dielectric tube on inductively coupled plasma source: Chamber structures and plasma characteristics

Zhen-Hua Bi(毕振华), Yi Hong(洪义), Guang-Jiu Lei(雷光玖), Shuai Wang(王帅), You-Nian Wang(王友年), Dong-Ping Liu(刘东平)
Chin. Phys. B, 2017, 26 (**7**): 075203. DOI: 10.1088/1674-1056/26/7/075203

Plasma potential measurements using an emissive probe made of oxide cathode

Jian-Quan Li(李建泉)[1,2], Hai-Jie Ma(马海杰)[1,2], and Wen-Qi Lu(陆文琪)[3,†]

[1] *Department of Electronic and Communication Engineering, North China Electric Power University, Baoding* 071003, *China*
[2] *Hebei Key Laboratory of Power Internet of Things Technology, North China Electric Power University, Baoding* 071003, *China*
[3] *Key Laboratory of Materials Modification by Laser, Ion and Electron Beams, School of Physics, Dalian University of Technology, Dalian* 116024, *China*

(Received 27 October 2023; revised manuscript received 11 December 2023; accepted manuscript online 22 December 2023)

A novel emissive probe consisting of an oxide cathode coating is developed to achieve a low operating temperature and long service life. The properties of the novel emissive probe are investigated in detail, in comparison with a traditional tungsten emissive probe, including the operating temperature, the electron emission capability and the plasma potential measurement. Studies of the operating temperature and electron emission capability show that the tungsten emissive probe usually works at a temperature of 1800 K–2200 K while the oxide cathode emissive probe can function at about 1200 K–1400 K. In addition, plasma potential measurements using the oxide cathode emissive probe with different techniques have been accomplished in microwave electron cyclotron resonance plasmas with different discharge powers. It is found that a reliable plasma potential can be obtained using the improved inflection point method and the hot probe with zero emission limit method, while the floating point method is invalid for the oxide cathode emissive probe.

Keywords: emissive probe, oxide cathode, plasma potential, filament temperature

PACS: 52.70.–m, 52.70.Ds, 79.40.+z **DOI:** 10.1088/1674-1056/ad1821

1. Introduction

An emissive probe is an effective and widely used tool for the measurement of space potential in a variety of environments including plasmas and vacuums.[1–5] The crucial component of an emissive probe is a thermionic cathode filament, which can produce a significant number of thermoelectrons when it is heated using a DC power or a laser source.[5–7] According to emissive probe theories, an accurate space potential can be determined from changes in the electron emission current.[8] Up to now, the most common thermionic material in emissive probes is tungsten filaments, which are also widely used in various electronic devices and systems such as vacuum tubes and electron guns.[9,10] However, the operating temperature of a tungsten filament is usually above 2200 K, and a tungsten filament in an incandescent state is always accompanied by intense evaporation loss.[11] As a result, the tungsten filament becomes thinner and thinner and its service life becomes shorter and shorter, which can inevitably affect the measurement results of plasma potential using a tungsten emissive probe.[11] The short life of a tungsten filament can also severely restrict application of the emissive probe in situations where the emissive probe is required to work continuously for a long time, such as in measurements of space potential distribution and plasma sheath structure. Some filaments are made with other cathode materials such as thoriated tungsten wires and LaB_6.[6,7,12–16] These cathode materials usually have a lower work function ($\sim$ 2.5 eV) and operating temperature ($\sim$ 1900 K) than tungsten (4.55 eV), which can reduce the need for heating energy and extend the longevity of filaments to some extent.[6,7,12,15,16] However, in practical applications, thoriated tungsten has been developed mainly as an electron source with a high thermionic emission, and it requires a cumbersome activation process before it can be used;[12,15] LaB_6 emissive probes are usually made into a tip rather than a filament and are often used with laser heating.[6,7]

In this work, a novel emissive probe made with an oxide cathode is proposed to achieve an emissive probe with a low operating temperature and long service life. With a lower work function, the operating temperature of the novel emissive probe is proved to be about 700 K lower than that of a conventional tungsten emissive probe. The reliability of the novel emissive probe for plasma potential measurements has also been investigated with different emissive probe techniques in microwave electron cyclotron resonance (MW-ECR) plasmas with different discharge powers. Compared with the plasma potential measured by a traditional tungsten emissive probe, it is demonstrated that the improved inflection point (IIP) method and the hot probe with zero emission limit (HP-ZEL) method are effective for the novel emissive probe, while the floating point (FP) method is invalid for plasma potential measurements.

2. Different emissive probe techniques

The emissive probe techniques used by us for plasma potential measurements are the IIP method,[3–5] the FP method[17–19] and the HP-ZEL method.[20] The IIP method is

†Corresponding author. E-mail: luwenqi@dlut.edu.cn

© 2024 Chinese Physical Society and IOP Publishing Ltd

devoted to finding the approximately linear relation between the inflection point potential of the emissive probe I–V traces (V_{ip}) and the probe heating current (I_{ht}) to avoid the influence of space-charge effects (also called the 'virtual cathode') caused by the emitted electrons on the plasma potential results. Performance of the IIP method requires the acquisition of a series of I–V traces with different electron emission currents (I_{emis}), finding the V_{ip}–I_{ht} relation, and then linearly extrapolating it to the limit of the particular heating current at which electron emission is initiated to obtain an accurate plasma potential. The FP method is based on the fact that the floating potential (V_f) of a strong electron-emitting filament approaches the plasma potential. Strict implementation of the FP method also requires the collection of a series of I–V curves and finding the V_f–I_{ht} relation; then the saturated floating potential (V_{sf}) is considered to be approximately equal to the plasma potential. In addition, we propose using the HP-ZEL method to easily obtain the accurate plasma potential and other reliable plasma parameters using the emissive probe;[20] this is essentially more of a Langmuir probe technique. The HP-ZEL method first requires finding the specified probe heating current for initial emission ($I_{ht\text{-}0emis}$) and then V_{ip} of the probe I–V trace acquired with $I_{ht\text{-}0emis}$ ($V_{ip\text{-}0emis}$) is considered to be the accurate plasma potential.

3. Experimental setup

All experiments were carried out in a multipurpose MW-ECR plasma setup,[20] as shown schematically in Fig. 1. The main vacuum chamber is made of stainless steel and is cylindrical in shape with an inner diameter of 60 cm and a depth of 80 cm. A cylindrical discharge chamber (15 cm inner diameter, 20 cm depth) surrounded by an electric coil is designed on each side of the main vacuum chamber for the generation of MW-ECR plasma. By setting the current directions of the two electric coils, two magnetic field patterns (mirror field and cusp field) can be obtained in the main vacuum chamber. In plasma diagnostic experiments, the cusped magnetic field is often used to obtain a uniform plasma without interference from the magnetic field in the chamber center.[20] In all experiments, the chamber was exhausted to a pressure baseline of 3.0×10^{-3} Pa and then filled with Ar gas up to 0.16 Pa. An ECR source was set at one side of the vacuum chamber where the plasma was produced and then transported to the main chamber. The typical MW power was chosen to be 300 W, 500 W, and 700 W.

Figure 2 shows a detailed schematic and a photograph of the emissive probe structure designed by us. The core component of the oxide cathode emissive probe is an ultrafine tungsten filament of diameter 20 μm and length 10 mm, and the middle 5 mm or so of the filament is evenly coated with an oxide cathode paste. The oxide cathode paste used here is

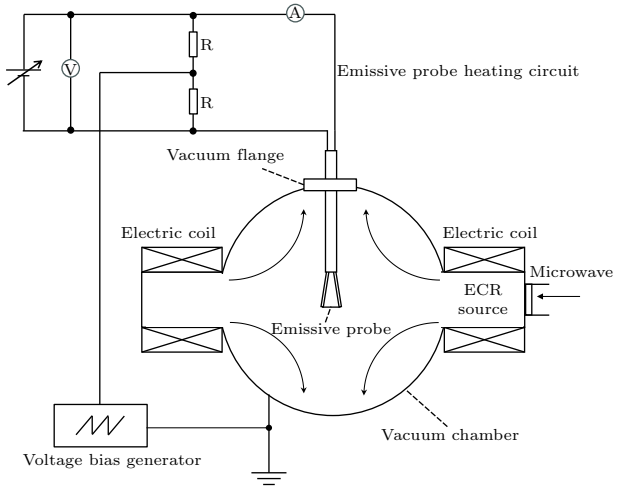


Fig. 1. Schematic diagram of the experimental device for plasma potential measurements using an emissive probe in MW-ECR plasmas.

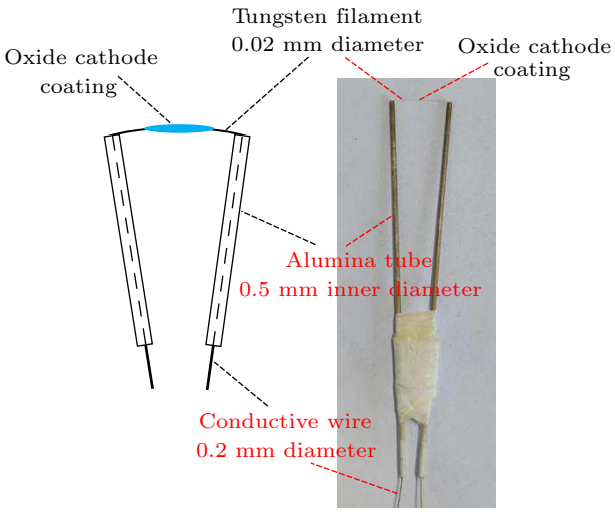


Fig. 2. Schematic diagram (left) and the photo (right) of construction of the oxide cathode emissive probe.

a commercial product that can be easily purchased; its main ingredient is a ternary carbonate with the molecular formula $(Ba,Sr,Ca)CO_3$, which can be heated to decompose into BaO, SrO and CaO. Of the three oxide materials, BaO has the lowest work function of 1.65 eV and is therefore the main electron emission material for the oxide cathode emissive probe. With its lower work function, a BaO cathode is often used as an electron source to obtain stable and long-lasting electron emission.[21,22] Note that the oxide cathode coating used here is so thin that it is difficult to see clearly in the photograph. Before the oxide cathode emissive probe was used for the first time it was heated continuously for 10 min with I_{ht} of 120 mA to ensure that the ternary carbonate can be completely decomposed. The tungsten filament was connected to the probe heating circuit through two ceramic-tube-covered conductive wires (tungsten, 0.2 mm in diameter), as shown in Figs. 1 and 2. In order to minimize the influence of the emissive probe on the plasma, the probe holders (two alumina tubes) were made especially small with an inner diameter of 0.5 mm and an outer

diameter of 1 mm. Additionally, the probe bias was applied between the filament and the grounded chamber through two sampling resistors in series, as shown in Fig. 1. As the filament impedance was only several Ohms, the potential drop across the filament was small and negligible.[4]

To evaluate the reliability of the plasma potential measurements performed by the oxide cathode emissive probe we also used a traditional tungsten emissive probe of the same size except for the absence of the oxide cathode coating to measure the same MW-ECR plasma. All emissive probe *I*–*V* curves were measured by the automatic emissive probe apparatus developed by us.[23,24] In this apparatus, the *I*–*V* curves were measured point to point, from low potential to high potential, with each point obtained from an average of 500 measurements in order to suppress the circuit noise and improve measurement precision.[5,25] Moreover, in the program for the apparatus, the usual heating current step and the scanning bias step of the emissive probe were respectively set to be 1 mA and 0.2 V.

4. Measurement results and discussion

4.1. Results for the filament temperature

It is necessary to obtain reliable filament temperatures (T) because one of the advantages of the oxide cathode emissive probe is its lower operating temperature. In a recently published paper we showed that the temperature of the emissive probe can be accurately measured with a two-color pyrometer.[11] However, for an ultrafine filament cathode with a diameter of the order of microns, a two-color pyrometer only works effectively when T exceeds 1700 K.[11] On the other hand, when the probe holders at both ends of the filament are very thin and the filament temperature is high, the heat conduction loss of the filament through the conductive wires is negligible. Therefore, we can use the Stefan–Boltzmann law to obtain a reliable filament temperature, as demonstrated in our previous paper.[26] The Stefan–Boltzmann law is described as[27,28]

$$U_{\rm ht}I_{\rm ht} = S\xi\sigma T^4, \tag{1}$$

where $U_{\rm ht}$ is the probe heating voltage, S is the whole surface area of the filament, ξ is the thermal emissivity, also called the radiation coefficient, and σ is the Stefan–Boltzmann constant, which is equal to 5.67×10^{-8} W·m^{-2}·K^{-4}.

According to the available literature and our experimental results,[11,29] ξ of the tungsten filament is usually between 0.1 and 0.4, corresponding to a T of 800 K–3000 K. Since we only want to obtain a reliable estimate for T and not achieve its accurate measurement, here we choose a median value of ξ (0.25) to calculate T. Using $U_{\rm ht}$ measured in a vacuum with a pressure of 3.0×10^{-3} Pa, figure 3 shows the estimated T of the tungsten filament with different $I_{\rm ht}$, suggesting that as $I_{\rm ht}$ increases, T increases monotonically from room temperature (300 K) to 2600 K.

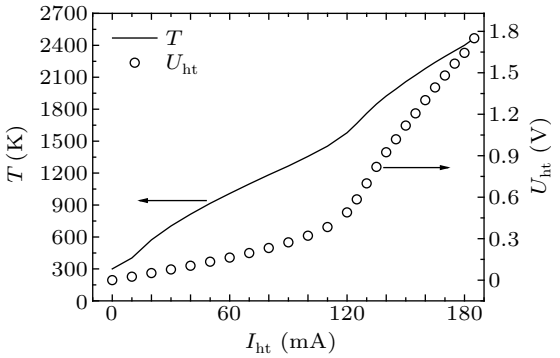


Fig. 3. Changes of the measured $U_{\rm ht}$ and the estimated T with different $I_{\rm ht}$ in a vacuum with a pressure of 3.0×10^{-3} Pa. T was calculated with $\xi = 0.25$.

4.2. Results for the electron emission current

Figure 4 shows the *I*–*V* curves obtained in a MW-ECR plasma using the oxide cathode emissive probe with different $I_{\rm ht}$. Using the measured *I*–*V* curves, $I_{\rm emis}$ is determined as the average of the probe current when the probe voltage is below −8 V and $V_{\rm ip}$ is defined as the maximum of the first derivative curve of the probe *I*–*V* trace, as shown in Fig. 4. The obvious increase in probe current under negative bias with $I_{\rm ht} = 94$ mA means that the emissive probe has a significant electron emission. Additionally, it is worth noting that with increase in $I_{\rm ht}$ and T, the electron collection current obtained by the oxide cathode emissive probe also increases, which is inconsistent with the phenomenon of plasma diagnostics using a traditional tungsten emissive probe. The change in the electron collection current may result from a change in the effective electron collection area of the oxide cathode emissive probe; we speculate that this may be due to the semiconductor characteristic of the oxide cathode (BaO). Besides, adsorptions and contaminations on the probe surface caused by the porous structure of the oxide cathode coating can also lead to changes in the effective electron collection area of the emissive probe. Compared with the traditional tungsten emissive probe, it is very challenging to obtain the reliable electron temperature and electron density of plasmas using the oxide cathode emissive probe.

Figure 5 shows the $I_{\rm emis}$–$I_{\rm ht}$ curves obtained by the oxide cathode emissive probe and the traditional tungsten emissive probe in an identical MW-ECR plasma. Combined with Fig. 3, we find that the electron emission of the oxide cathode emissive probe is initiated at $I_{\rm ht} = 90$ mA with a corresponding T of about 1200 K, while the electron emission of the traditional tungsten emissive probe is initiated at $I_{\rm ht} = 134$ mA with a corresponding T of about 1800 K. Moreover, the oxide cathode emissive probe and the traditional tungsten emissive probe can produce an appreciable electron emission with T equal

to about 1400 K and 2200 K, respectively. The results agree well with the electron emission properties of the tungsten cathode and BaO cathode reported in the published literature,[11,22] indicating that our estimate of T is reliable. The difference between the operating temperature (about 700 K) of the two probes suggests the great advantage of the oxide cathode emissive probe in operating at lower temperature and saving energy. Reduction of the operating temperature can also greatly reduce the evaporation loss of tungsten filaments. Since the manufacturing process of the traditional emissive probe is not easy, the use of the novel emissive probe is very convenient because there is no need to frequently replace the tungsten filament.

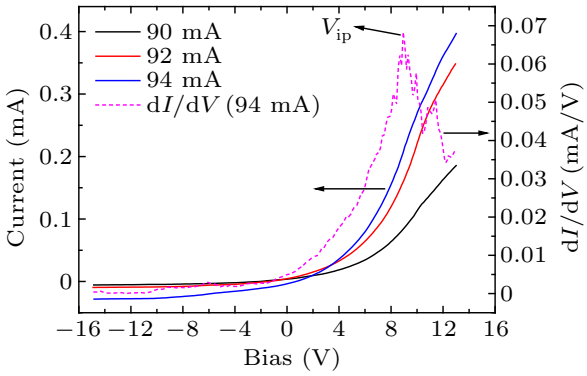


Fig. 4. The I–V curves measured by the oxide cathode emissive probe in a MW-ECR plasma with different I_{ht} (90 mA, 92 mA, and 94 mA), together with the first derivative curve of the I–V trace obtained with $I_{ht} = 94$ mA. The MW power was 500 W, and the electric coil current was set to be 78 A to obtain a cusped magnetic field.

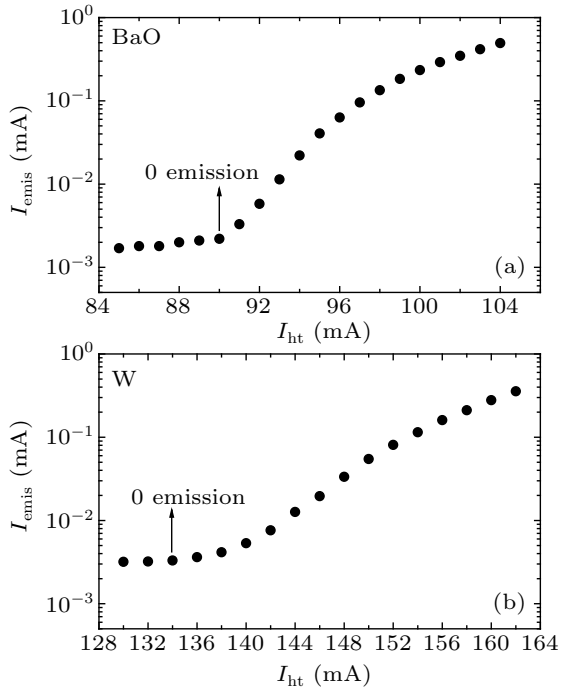


Fig. 5. Variations of I_{emis} with I_{ht} obtained with (a) the oxide cathode emissive probe and (b) the traditional tungsten emissive probe. The MW power was 500 W, and the electric coil current was set to be 78 A to obtain a cusped magnetic field.

4.3. Results for the plasma potential

Figure 6 shows the V_{ip}–I_{ht} curves and the V_f–I_{ht} curves obtained by the oxide cathode emissive probe and the traditional tungsten emissive probe in an identical MW-ECR plasma with a MW power of 500 W. As the traditional tungsten emissive probe begins to emit electrons at $I_{ht} = 134$ mA, V_{ip} decreases approximately linearly from 10.20 V to 9.87 V under the influence of the virtual cathode, while V_f increases monotonically from 0.73 V and eventually tends to saturation at about 9.86 V. On the other hand, as the oxide cathode emissive probe begins to emit electrons at $I_{ht} = 90$ mA, V_{ip} drops roughly linearly from 10.06 V to 6.42 V, while V_f increases monotonically from −2.20 V and eventually tends to saturation at about 5.99 V. Using the IIP method by linear fitting of the V_{ip}–I_{ht} curves, the plasma potentials determined by the oxide cathode emissive probe and traditional tungsten emissive probe are 10.50 V and 10.25 V, respectively. Using the HP-ZEL method by finding V_{ip} of the probe I–V trace acquired with $I_{ht\text{-}0emis}$, the plasma potentials determined by the oxide cathode emissive probe and the traditional tungsten emissive probe are 10.06 V and 10.20 V, respectively. Using the FP method by finding V_{sf}, the plasma potentials obtained by the oxide cathode emissive probe and the traditional tungsten emissive probe are 5.99 V and 9.86 V, respectively.

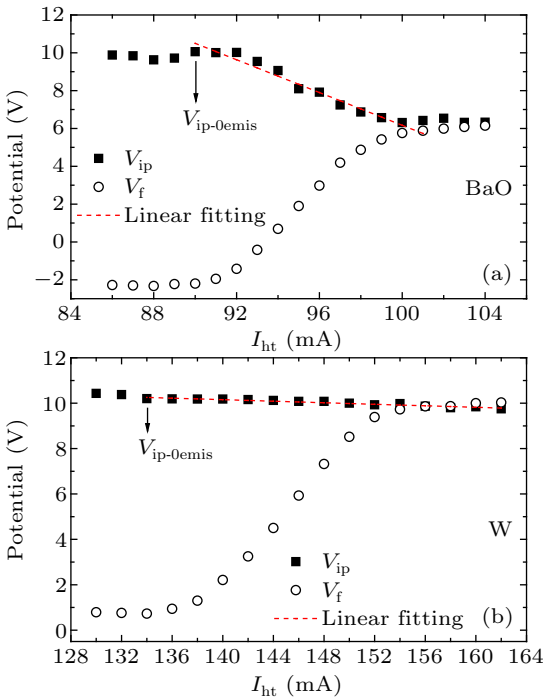


Fig. 6. Variations of V_{ip} and V_f with I_{ht} obtained by (a) the oxide cathode emissive probe and (b) the traditional tungsten emissive probe. The MW power was 500 W, and the electric coil current was set to be 78 A to obtain a cusped magnetic field.

To increase the reliability of the measurement results, we conducted several repeated measurements, and the final results for the plasma potential determined by the two probes using the different methods are shown in Fig. 7. In our previous

studies we demonstrated that the plasma potential obtained by the IIP method (V_p) is the most accurate result.[4,20] Therefore, using both the IIP method and the HP-ZEL method the oxide cathode emissive probe can produce reliable results for the plasma potential, but the plasma potential result obtained with the FP method using the oxide cathode emissive probe is significantly lower than the actual plasma potential. The plasma potential result obtained with the IIP method using the traditional tungsten emissive probe (V_{p-W}) can be considered as the actual plasma potential of about 10.33 V. Further, we use the relative difference of the potential (δ_p) to describe the relation between V_{p-W} and the plasma potential results ($V_{x\text{-BaO}}$) obtained by the oxide cathode emissive probe using different methods. Hence, δ_p can be calculated as

$$\delta_p = \frac{V_{p-W} - V_{x\text{-BaO}}}{V_{p-W}} \times 100\%. \quad (2)$$

As shown in Fig. 7, although the relative difference between V_{p-W} and the plasma potential results obtained by the oxide cathode emissive probe using the IIP method and the HP-ZEL method is small (only about 3%), there is a huge difference of more than 40% between V_{p-W} and the plasma potential results obtained with the oxide cathode emissive probe using the FP method. In our recent studies of the virtual cathode caused by emissive probes we found that the potential and size of the virtual cathode is closely related to T.[26,30] Therefore, combined with Figs. 3, 5 and 6, the main reasons for the failure of the FP method with the oxide cathode emissive probe can be explained as follows. On the one hand, the oxide cathode is made of semiconductor material and has a high resistance, so the oxide coating on the tungsten filament can capture a high voltage drop, resulting in a lower value of V_f determined by the probe. On the other hand, at the same electron emission intensity, the lower the filament temperature, the lower the initial energy of the electrons emitted by the cathode, and the more electrons that will gather near the cathode surface, eventually forming a larger virtual cathode. The larger virtual cathode causes V_{ip} to move further toward the lower potential and prevents the increase of V_f, as shown in Fig. 6. In the end, the combined effect of the two results leads to the values of V_{sf} measured by the oxide cathode emissive probe being significantly lower than those determined by the traditional tungsten emissive probe. This is also the main reason why the slope of the linear fitting of the V_{ip}–I_{ht} curve shown in Fig. 6(a) is greater than that shown in Fig. 6(b). Additionally, it is worth noting that the larger slope of the linear fitting of the V_{ip}–I_{ht} curve also leads to a large uncertainty in the plasma potential results determined by the IIP method with the oxide cathode emissive probe. Therefore, the most suitable technique for plasma potential measurement using the oxide cathode emissive probe may be the HP-ZEL method.

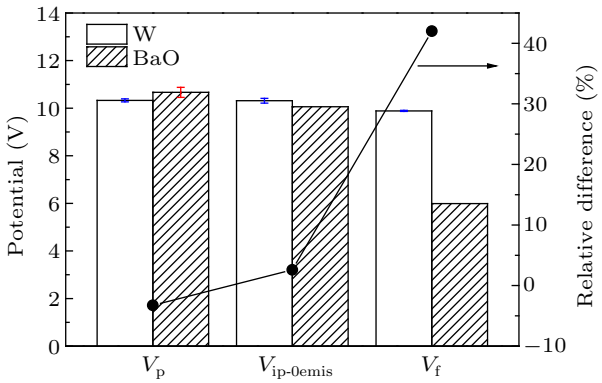


Fig. 7. The plasma potential results determined by the two probes using different methods, together with the relative difference between the actual plasma potential (10.33 V) and the plasma potential results ($V_{x\text{-BaO}}$) obtained by the oxide cathode emissive probe using different methods. The plasma potential results obtained by using the IIP, HP-ZEL and FP methods are expressed as V_p, $V_{ip\text{-}0emis}$ and V_{sf}, respectively.

4.4. Results for the plasma potential measured in MW-ECR plasmas with different discharge powers

Figure 8 shows the V_{ip}–I_{ht} curves and V_f–I_{ht} curves obtained by the oxide cathode emissive probe and the traditional tungsten emissive probe in an identical MW-ECR plasma with a MW power of 300 W. Using the IIP method, the actual plasma potential is determined to be 7.75 V and 7.49 V, respectively, with the traditional tungsten emissive probe and oxide cathode emissive probe. Using the HP-ZEL method, the plasma potential is found to be 7.79 V and 7.68 V, respectively, by the two probes. Using the FP method, the plasma potential is found to be 7.30 V and 4.20 V, respectively, by the two probes. Figure 9 shows the V_{ip}–I_{ht} curves and V_f–I_{ht} curves obtained by the oxide cathode emissive probe and traditional tungsten emissive probe in an identical MW-ECR plasma with a MW power of 700 W. Using the IIP method, the actual plasma potential is determined to be 11.36 V and 11.32 V, respectively, by the traditional tungsten emissive probe and the oxide cathode emissive probe. Using the HP-ZEL method, the plasma potential is found by the two probes to be 11.34 V and 11.39 V, respectively. Using the FP method, the plasma potential is found by the two probes to be 10.65 V and 7.19 V, respectively.

Table 1 shows the plasma potential results after at least three repetitions as determined by the oxide cathode emissive probe and the traditional tungsten emissive probe using

Table 1. The plasma potential results determined by the two probes using different methods in MW-ECR plasmas with MW powers of 300 W, 500 W and 700 W. These results were replicated at least three times and then averaged.

MW power (W)	Oxide cathode probe			Tungsten probe		
	V_p (V)	$V_{ip\text{-}0emis}$ (V)	V_{sf} (V)	V_p (V)	$V_{ip\text{-}0emis}$ (V)	V_{sf} (V)
300	7.48	7.68	4.19	7.74	7.79	7.30
500	10.67	10.06	5.99	10.33	10.31	9.89
700	11.62	11.40	7.18	11.30	11.34	10.64

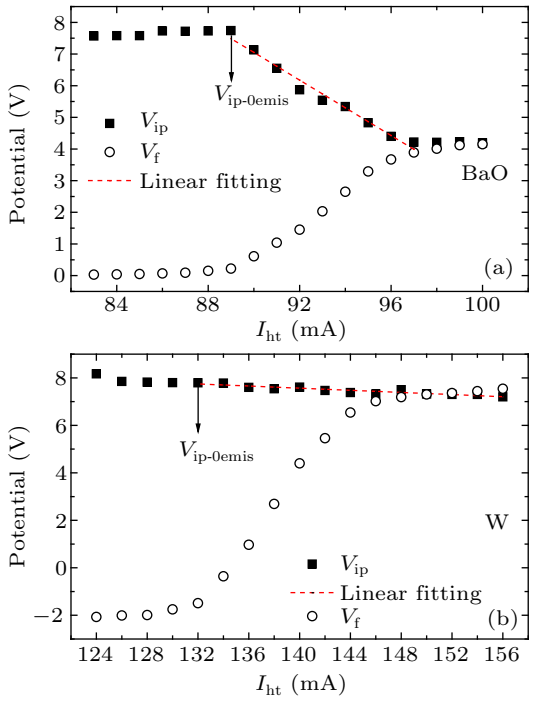


Fig. 8. Variations of V_{ip} and V_f with I_{ht} obtained by (a) the oxide cathode emissive probe and (b) a traditional tungsten emissive probe. The MW power was 300 W and the electric coil current was set to be 100 A to obtain a cusped magnetic field.

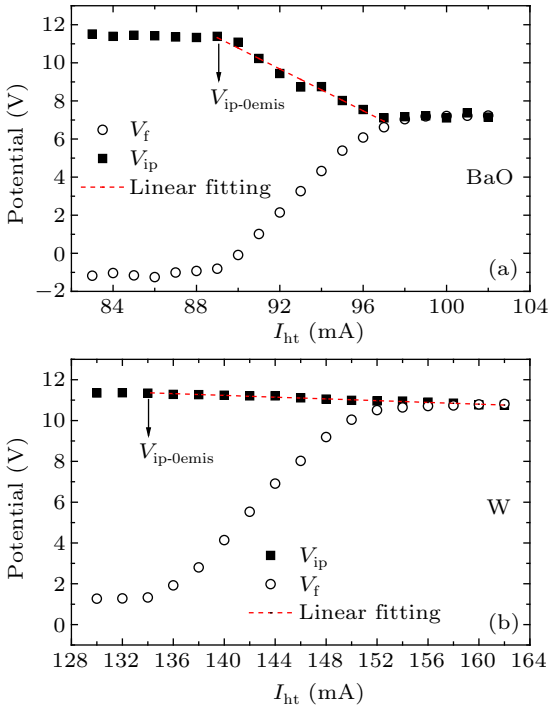


Fig. 9. Variations of V_{ip} and V_f with I_{ht} obtained by (a) the oxide cathode emissive probe and (b) the traditional tungsten emissive probe. The MW power was 700 W, and the electric coil current was set to be 103 A to obtain a cusped magnetic field.

different methods in MW-ECR plasmas with different MW powers. We have demonstrated that the most reliable results for plasma potential measurements are those obtained by the traditional tungsten emissive probe with the IIP method.[4,20] Hence, the plasma potential of MW-ECR plasmas with MW powers of 300 W, 500 W, and 700 W can be considered to be 7.74 V, 10.33 V, and 11.30 V, respectively. Further, using Eq. (2), we can obtain the relative difference (δ_p) between the standard results and the plasma potential results determined by the oxide cathode emissive probe using different methods. For a MW-ECR plasma with a MW power of 300 W, δ_p is calculated to 3.36%, 0.78%, and 45.87%, corresponding to the IIP method, the HP-ZEL method and the FP method, respectively. For the MW-ECR plasma with a MW power of 500 W, δ_p is calculated to 3.29%, 2.61%, and 42.01%, respectively, for the IIP method, the HP-ZEL method and the FP method. For the MW-ECR plasma with a MW power of 700 W, δ_p is calculated to 2.83%, 0.88%, and 36.46%, corresponding to the IIP method, the HP-ZEL method and the FP method, respectively. Comparing δ_p, we find that it is effective to measure the plasma potential using the oxide cathode emissive probe with the IIP method and the HP-ZEL method. The huge difference of about 40% suggests that plasma potential cannot be measured using the oxide cathode emissive probe with the FP method.

5. Conclusion

To reduce the operating temperature and prolong the service life of emissive probes, a novel emissive probe is proposed by coating an oxide cathode (BaO) on the surface of a tungsten filament. The oxide cathode emissive probe has been investigated in terms of its operating temperature, electron emission performance and plasma potential measurement and compared with the traditional tungsten emissive probe. Using the Stefan–Boltzmann law to estimate T, it is found that the oxide cathode emissive probe can produce electron emission at about 1200 K while the traditional tungsten emissive probe requires a temperature of 1800 K. When considerable electron emission is generated, T of the oxide cathode emissive probe is about 1400 K while emission in the traditional tungsten cathode emissive requires a temperature of 2200 K. We also carried out comparative measurements of the plasma potential with the oxide cathode emissive probe and the traditional tungsten emissive probe in MW-ECR plasmas with different discharge powers. Using the IIP method and HP-ZEL method, the plasma potential results determined by the oxide cathode emissive probe are in good agreement with the actual plasma potential. However, there is a huge difference between the actual plasma potential and the results determined by the FP method using the oxide cathode emissive probe, suggesting that it fails to obtain an accurate plasma potential using the novel emissive probe with the FP method. The reason for this thought to be that for the same electron emission intensity, the virtual cathodes formed near the surface of the oxide cathode emissive probe are larger than those formed near the

surface of the traditional tungsten emissive probe. The development of the novel emissive probe featuring a low operating temperature and long service life is of great significance for measurements of space potential distribution, such as the experimental study of the plasma sheath structure using emissive probes.

Acknowledgments

Project supported by the National Natural Science Foundation of China (Grant No. 11905076) and S&T Program of Hebei (Grant No. SZX2020034).

References

[1] Oksuz L and Hershkowitz N 2002 *Phys. Rev. Lett.* **89** 145001
[2] Sheehan J P and Hershkowitz N 2011 *Plasma Sources Sci. Technol.* **20** 063001
[3] Li J Q, Xu J, Bai Y J, Lu W Q and Wang Y N 2016 *J. Vac. Sci. Technol. A* **34** 061304
[4] Li J Q, Lu W Q, Xu J, Gao F and Wang Y N 2018 *Vacuum* **155** 566
[5] Li J Q, Lu W Q, Xu J and Gao F 2019 *Plasma Phys. Contr. Fusion* **61** 105005
[6] Schrittwieser R, Ionita C, Balan P, Gstrein R, Grulke O, Windisch T, Brandt C, Klinger T, Madani R, Amarandei G and Sarma A K 2008 *Rev. Sci. Instrum.* **79** 083508
[7] Kella V P, Mehta P, Sarma A, Ghosh J and Chattopadhyay P K 2016 *Rev. Sci. Instrum.* **87** 043508
[8] Ye M Y and Takamura S 2000 *Phys. Plasma.* **7** 3457
[9] Hadley C P 1953 *J. Appl. Phys.* **24** 49
[10] Fan J K, Peng Y, Xu J Q, Xu H Y, Yang D Q, Li X P and Zhou Q 2019 *Vacuum* **164** 278
[11] Li J Q, Li S H and Liu P 2023 *Vacuum* **210** 111837
[12] Lafferty J M and Kingdon K H 1946 *J. Appl. Phys.* **17** 894
[13] Horsting C W 1947 *J. Appl. Phys.* **18** 95
[14] Fan H Y 1949 *J. Appl. Phys.* **20** 682
[15] Schneider P 1958 *J. Chem. Phys.* **28** 675
[16] Murray R G and Collier R J 1977 *Rev. Sci. Instrum.* **48** 870
[17] Kemp R F and Sellen J M 1966 *Rev. Sci. Instrum.* **37** 455
[18] Yamada H and Murphree D L 1971 *Phys. Fluids* **14** 1120
[19] Sheehan J P, Raitses Y, Hershkowitz N, Kaganovich I and Fisch N J 2011 *Phys. Plasma* **18** 073501
[20] Li J Q, Zhang Q H, Xing Z Y and Lu W Q 2022 *J. Vac. Sci. Technol. A* **40** 033001
[21] Davies D E and Hopkins B J 1959 *Br. J. Appl. Phys.* **10** 498
[22] Fang H K, Oyama K I and Chen A B 2017 *Plasma Sources Sci. Technol.* **26** 115010
[23] Li J Q, Lu W Q, Xu J, Gao F and Wang Y N 2017 *Rev. Sci. Instrum.* **88** 115106
[24] Li J Q, Lu W Q, Xu J, Gao F and Wang Y N 2018 *Plasma Sci. Technol.* **20** 024002
[25] Lu W Q, Jiang X Z, Liu Y X, Yang S, Zhang Q Z, Li X S, Xu Y, Zhu A M and Wang Y N 2013 *Plasma Sci. Technol.* **15** 511
[26] Li J Q, Xie X Y, Li S H and Zhang Q H 2022 *Vacuum* **200** 111013
[27] LoPresto M C and Hagoort N 2011 *Phys. Teach.* **49** 113
[28] Carlá M 2013 *Am. J. Phys.* **81** 512
[29] Bramson M A 1968 *Infrared Radiation: A Handbook for Applications, Optical Physics & Engineering*, New York Plenum Press, New York, 1968, p. 536
[30] Li S H and Li J Q 2021 *Vacuum* **192** 110496